Invited Paper

Precise open-loop control of MEMS deformable mirror shape

Thomas Bifano [a,c], Jason Stewart [b], Alioune Diouf [c]

[a] Boston University Photonics Center, 8 Saint Mary's St., Boston, MA 02215, tgb@bu.edu
[b] Dept. of Electrical and Computer Eng., 8 Saint Mary's St., Boston, MA 02215, jstew@bu.edu
[c] Dept. of Manufacturing Eng., 15 Saint Mary's St., Brookline, MA 02446, alioune@bu.edu

ABSTRACT

A new method is introduced for predicting control voltages that will generate a prescribed surface shape on a deformable mirror. The algorithm is based upon an analytical elastic model of the mirror membrane and an empirical electromechanical model of its actuators. It is computationally simple and inherently fast. Shapes at the limit of achievable mirror spatial frequencies with up to 1.5µm amplitudes have been achieved with less than 15nm RMS error.
Keywords: MEMS, adaptive optics, open-loop control, deformable mirror

1. INTRODUCTION

In some imaging applications optical aberrations inherent to the imaging optics or beam path degrade image resolution and contrast. Image quality improvements can be achieved by altering the wavefront in a way that counteracts the effects of aberrations. In its simplest form, such an adaptive optics controller consists of a wavefront sensor, a deformable mirror (DM), and a real-time control system that links the two, imposing on the DM a shape that complements the wavefront error, with half its amplitude.

The deformable mirror must be capable of approximating the system's expected wavefront error, including its amplitude, spatial distribution, and time rate of change. When the expected wavefront errors include large spatial and temporal frequencies, in large, ground-based astronomical telescopes for example, the deformable mirrors need correspondingly more and faster actuators. DMs made using microelectromechanical systems (MEMS) technology have inherent advantages in such applications when compared to mechanically assembled DMs due to their scalability to large actuator arrays, and to their fast response. One particular MEMS DM architecture suitable for adaptive optics control on large ground-based telescopes was pioneered at Boston University. These MEMS DMs have demonstrated sub-nanometer positioning precision, repeatability and stability [1,2].

In most large telescope AO applications, closed-loop control using wavefront error feedback is used to improve image quality. High precision is achieved by iteratively monitoring the difference between current and desired mirror shapes, and using this error signal to drive the mirror into an increasingly better shape. One instrumentation concept for such large telescopes – multi-object adaptive optics (MOAO) – places an additional burden on the DM: that it is controllable in shape to nanometer scale precision in a single step (i.e. without feedback). Such control is made plausible by the fact that the MEMS DM exhibits no measurable hysteresis. However, it is difficult to predict voltages required to achieve DM shapes in a precise open-loop manner due to the high degree of mechanical coupling between adjacent DM actuators through the mirror membrane. Further complicating the problem is the nonlinear relationship between applied voltage and deflection behavior of each electrostatic actuator.

Morzinski et al at the Laboratory for Adaptive Optics, University of California, Santa Cruz, have developed the most accurate open-loop control routine thus far using empirical and mathematical models [3]. The algorithm (based on measured actuator influence functions) predicted DM control voltages for 500nm amplitude mirror shapes with residual shape errors of about 15nm RMS.

MEMS Adaptive Optics II, edited by Scot S. Olivier, Thomas G. Bifano, Joel A. Kubby,
Proc. of SPIE Vol. 6888, 68880P, (2008) · 0277-786X/08/$18 · doi: 10.1117/12.769492

Downloaded from SPIE Digital Library on 09 Sep 2010 to 128.197.165.107. Terms of Use: http://spiedl.org/terms

A 300µm pitch DM with 2µm stroke and 144 actuators (12x12) was selected to demonstrate the open-loop control method presented here. The DM has an aperture diameter of 3.3mm, a facesheet thickness of 3µm and an actuator diaphragm thickness of 2µm. The actuator diaphragm is 230µm wide, has a 260µm span, and an electrostatic gap of 5µm. A schematic of the DM cross section (not to scale) is depicted in Figure 1.

2. MODEL AND EXPERIMENTS

Our model treats the DM as a system comprised of two mechanical subsystems: the continuous facesheet modeled as a thin plate undergoing both stretching and bending, and the array of actuators connected to the facesheet via rigid posts, modeled as fixed-fixed beams [4-7]. We determine all the forces involved in this system and perform a force balance at the posts, which are the point of connection for the two subsystems.

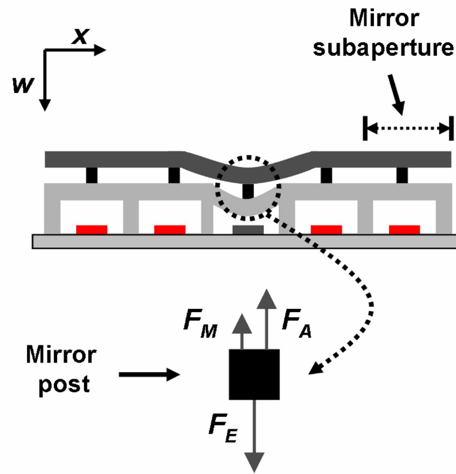

Figure 1: Cross section of an actuated DM subaperture (top) and free body diagram for its post (bottom). F_M is the mirror force, F_A is the actuator restoring force, and F_E is the applied electrostatic force.

The governing equation for out-of-plane deflections of a linear elastic plate is the biharmonic equation, which considers both bending and stretching:

$$\nabla^4 w(x,y) = \frac{q(x,y)}{D} + \frac{6}{h^2}\left\{\left[\left(\frac{\partial w(x,y)}{\partial x}\right)^2 \frac{\partial^2 w(x,y)}{\partial x^2}\right] + \left[\left(\frac{\partial w(x,y)}{\partial y}\right)^2 \frac{\partial^2 w(x,y)}{\partial y^2}\right]\right\} \quad \textbf{(1)}$$

with plate deflection w, flexural rigidity D, elastic modulus E, Poisson's ratio ν, surface normal load q, and plate thickness h. It assumes that the mirror facesheet only experiences surface normal forces and that any lateral forces can be neglected. It also assumes that there are no initial internal stresses in the facesheet. Using this equation the generalized load $q(x,y)$ necessary to create a desired (known) mirror shape $w(x,y)$ can be calculated. In reality however the mirror is loaded only at discrete points corresponding to the mirror post locations, and the generalized load can be represented by a collection of discrete forces F_M acting at these post locations. F_M is estimated at each post by integrating $q(x,y)$ over each DM subaperture.

To a first order the actuators can be modeled as a parallel-plate spring system. The top plate represents the compliant actuator diaphragm, which is attached to a spring representing the restoring force associated with its elastic displacement. The bottom plate represents the actuator's fixed electrode. In this model it is assumed that the plate representing the actuator diaphragm is infinitely rigid and that its stiffness is constant, similar to a linear spring. The actuator plate deflects due to an electrostatic force F_E that can be modeled as:

Downloaded from SPIE Digital Library on 09 Sep 2010 to 128.197.165.107. Terms of Use: http://spiedl.org/terms

$$F_E = \frac{\varepsilon_0 A V^2}{2(g_0 - w_p)^2} \quad , \qquad \textbf{(2)}$$

where w_p is the displacement of the actuator, ε_0 is the permittivity of free space, A is the plate area, V is the applied voltage and g_0 is the initial actuator gap. This force deforms the actuator plate, creating an actuator mechanical restoring force F_A that is (to first order, assuming constant stiffness k_A) proportional to the displacement of the actuator:

$$F_A = k_A w_p \,. \qquad \textbf{(3)}$$

The open-loop control architecture is based on a force balance at each actuator's centrally located post, with the simplifying assumption that the electrostatic force acts at a point instead of being distributed across the actuator plate. This assumption limits the ultimate precision of the approach, since the electrostatic force distribution across the actuator plate changes with increased deflection from one that is initially uniform to one that is concentrated near the actuator plate center. Balancing the forces for this model we find an analytical expression for actuator control voltages:

$$V_i = \sqrt{\frac{2(g_0 - w_{p,i})^2 (k_A w_{p,i} + F_{M,i})}{\varepsilon_0 A}} \quad , \qquad \textbf{(4)}$$

where the subscript i identifies a particular actuator. This demonstrates the dependence of actuator control voltage on its displacement *and* on forces coupled from the DM facesheet.

Unfortunately, the parallel-plate electrostatic model (2) and linear-spring mechanical model (3) provide relatively poor approximations of the actuator behavior. The actuator diaphragm is rigidly fixed along two opposing edges and not free as the model assumes. Such actuator diaphragm boundary conditions are referred to as "fixed-fixed." As a result the electrostatic model is limited by the fact that the electrodes are only parallel when the actuator is in its initial un-energized position. Therefore the electrostatic force distribution across the actuator diaphragm changes with increased deflection from one that is initially uniform to one that is concentrated near the diaphragm center. The mechanical model is also limited by stretching that effectively stiffens the actuator with increased deflection, i.e. k_A is not constant.

Open-loop control is still tractable however because the two forces F_A and F_E are local to the actuator, while global coupling is completely described through the mirror force F_M at each actuator post. Because of this, it is possible to reduce the open-loop control problem to one that is entirely local and uncoupled, provided that the mirror force F_M is known at each actuator. As a result, the electrostatic actuator response to a local mirror force F_M can be modeled through a compact set of empirical measurements with the functional relationship F_M = f(w_p,V), which is subject to the equilibrium condition:

$$F_M = F_A + F_E \,. \qquad \textbf{(5)}$$

The open-loop control approach presented here is therefore based on using a calibration step to find a local, empirical measure of the actuator behavior linking values of F_M, w_p and V, where w_p now refers to the displacement of the actuator post connection. The calibration table shown in Figure 2 (right) was created by applying identical voltages to a ring of actuators (left) to vary F_M at the central actuator. w_p(V) for the central actuator was then measured using a Zygo New View 6000 optical profiler for several ring voltages (or F_M's). F_M was calculated at each actuator using Equation (1). One hundred data points for F_M, w_p and V for a single actuator were recorded and least-squares fit to a surface of the same functional form as Equation (4). This surface was then used to predict the open-loop control voltages for the shape presented in Figure 3. Additional algorithm discussion and experimental results can be found in reference [8].

Downloaded from SPIE Digital Library on 09 Sep 2010 to 128.197.165.107. Terms of Use: http://spiedl.org/terms

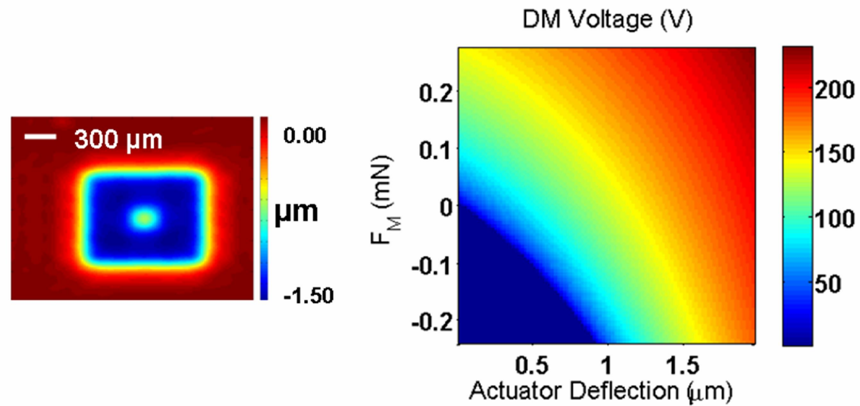

Figure 2: Shape used to calibrate DM (left). Identical voltages are applied to a ring of actuators to vary F_M at the central actuator. w_p(V) for the central actuator is measured for different ring voltages to produce the calibration dataset spanning $\{w_p, F_M, V\}$ (right). 100 data points from a single central actuator of the 12x12 DM were collected and fit to a surface of the same functional form as Equation (1). Surface fitting error was 4V RMS.

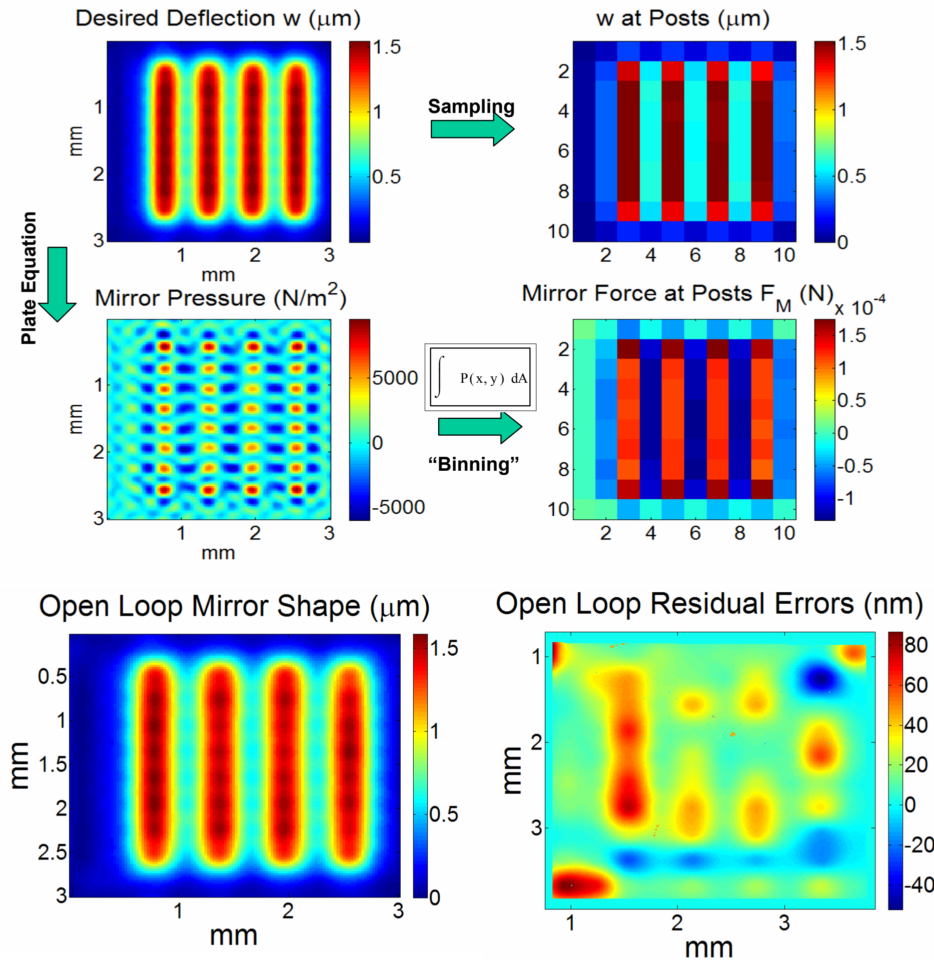

Figure 3: Open-loop prediction for a 1.5 µm amplitude (185 V) stripe pattern. The residual error between the desired shape (top left) and predicted shape (lower left) was 111 nm peak-to-valley and 13.5 nm rms (lower right). The other figure frames illustrate the control flow: the desired mirror shape is sampled (top right) to receive w_p, differentiated (middle left) and "binned" (middle right) to determine F_M, which are used to calculated the control voltage V from the surface in Figure 2.

Downloaded from SPIE Digital Library on 09 Sep 2010 to 128.197.165.107. Terms of Use: http://spiedl.org/terms

3. ACKNOWLEDGEMENTS

Portions of this work were supported by Army Research Lab contract W911NF-06-2-0040. Dr. Bifano acknowledges a financial interest in Boston Micromachines Corp., the manufacturer of the DM used in this study. The authors are grateful for support from D. Gavel and K. Morzinski, and for experiments performed by Janice Castillo and Andrew Legendre.

4. REFERENCES

[1] J. W. Evans, B. Macintosh, L. Poyneer, K. Morzinski, S.Severson, D. Dillon, D. Gavel, and L. Reza, “Demonstrating sub-nm closed-loop MEMS flattening,” Opt. Express **14**, 5558 (2006).
[2] K. M. Morzinski, J. W. Evans, S. Severson, B. Macintosh, D. Dillon, D. Gavel, C. Max, and D. Palmer, “Characterizing the potential of MEMS deformable mirrors for astronomical adaptive optics,” Proc. SPIE **6272**, 627221 (2006).
[3] K. M. Morzinski, K. B. W. Harpsee, D. T. Gavel, and S. M. Ammons, “The open-loop control of MEMS: modeling and experimental results,” Proc. SPIE **6467**, 64670G (2007).
[4] C. R. Vogel and Q. Yang, “Modeling, simulation, and open-loop control of a continuous facesheet MEMS deformable mirror,” J. Opt. Soc. Am. A **23**, 1074–1081 (2006).
[5] S. Timoshenko and S. Woinowsky-Krieger, Theory of Plates and Shells (McGraw-Hill, 1976), pp. 79–104 and 378–428.
[6] A. Papavasiliou, S. Olivier, T. Barbee, C. Walton, and M. Cohn, “MEMS actuated deformable mirror,” Proc. SPIE 6113, 190–199 (2006).
[7] S. D. Senturia, Microsystem Design (Springer Science, 2001), p. 134.
[8] J. B. Stewart, A. Diouf, Y. Zhou, and T.G. Bifano, “Open-loop Control of a MEMS Deformable Mirror for Large Amplitude Wavefront Control,” JOSA – A **24**(12), 3827-3833 (2007).

Downloaded from SPIE Digital Library on 09 Sep 2010 to 128.197.165.107. Terms of Use: http://spiedl.org/terms